J|A|C|S
ARTICLES
Published on Web 03/24/2005

Single-Molecule Tracing on a Fluidic Microchip for Quantitative Detection of Low-Abundance Nucleic Acids

Tza-Huei Wang,*,† Yahui Peng,† Chunyang Zhang,† Pak Kin Wong,‡ and Chih-Ming Ho‡

Contribution from the Department of Mechanical Engineering and Whitaker Biomedical Engineering Institute, Johns Hopkins University, 3400 North Charles Street, Baltimore, Maryland 21218, and Institute for Cell Mimetic Space Exploration (CMISE) and Department of Mechanical & Aerospace Engineering, University of California, Los Angeles, 420 Westwood Plaza, Los Angeles, California 90095

Received December 7, 2004; E-mail: thwang@jhu.edu

Abstract: Here, we report a method capable of quantitative detection of low-abundance DNA/RNA molecules by incorporating confocal fluorescence spectroscopy, molecular beacons, and a molecular-confinement microfluidic reactor. By using a combination of ac and dc fields via a trio of 3-D electrodes in the microreactor, we are able to precisely direct the transport of individual molecules to a minuscule laser-focused detection volume (~1 fL). A burst of fluorescence photons is detected whenever a molecular beacon−target hybrid flows through the detection region, and the amount of targets can be directly quantified according to the number of recorded single-molecule flow-through events. This assay consumes only attomoles of molecular probes and is able to quantitatively detect subpicomolar DNA targets. A measurement time of less than 2 min is sufficient to complete the detection.

Introduction

Qualitative and quantitative study of DNA/RNA is of great importance in many fields, such as disease diagnostics, gene expression studies, and drug discovery. However, conventional assays, including Southern Blotting and Northern Blotting, are time-consuming and incapable of detecting cases where only minute amounts of samples are available due to the lack of high sensitivity. Microarrays provide a high-throughput approach that detects a large number of genes in a single experiment; yet, detection at the cellular level using the array technique without sequence pre-amplification still remains a challenge. Polymerase chain reaction (PCR) enables the detection of low-quantity DNA/RNA after a large number of amplification cycles. The quantitative applications of this method, however, may suffer from complications due to background amplification and variances in amplification efficiency.[1,2] Hence, a great deal of effort still needs to be taken in order to enhance the sensitivity and speed of nucleic acid detection and quantification while at the same time help to validate the quantitative reliability of the available techniques.

Advances in confocal optics and fluorescence techniques have enabled detection of single-molecule fluorescence in solutions.[3−6] When incorporating fluorescently labeled molecular probes, the confocal single-molecule detection technique provides an alternative way for ultrasensitive biomolecule detection that has great potential for highly accurate, quantitative study of non-amplified targets. The technique is based on the use of confocal fluorescence spectroscopy, which detects the photons emitted from a fluorescent molecule when it diffuses through a miniscule laser-illuminated region (~1 fL). The small detection volume significantly reduces the background noise originating from spurious fluorescence of impurities and Raman scattering of solvent molecules, so that the signal-to-noise ratio (SNR) is maximized and ultrahigh sensitivity is achieved. The confocal single-molecule technique has been used for fundamental studies, such as molecular binding and interactions,[7−11] as well as for practical applications, such as nucleic acid detection,[12−14] gene expression study,[9] and DNA sequencing.[15] Despite these advances, full utilization of the unique advantages of single-molecule detection for biomolecule quantification to achieve

† Johns Hopkins University.
‡ University of California, Los Angeles.

(1) Halford, W. P.; Falco, V. C.; Gebhardt, B. M.; Carr, D. J. J. *Anal. Biochem.* **1999**, *266*, 181−191.
(2) Peccoud, J.; Jacob, C. *Biophys. J.* **1996**, *71*, 101−108.
(3) Barnes, M. D.; Ng, K. C.; Whitten, W. B.; Ramsey, J. M. *Anal. Chem.* **1993**, *65*, 2360−2365.
(4) Shera, E. B.; Seitzinger, N. K.; Davis, L. M.; Keller, R. A.; Soper, S. A. *Chem. Phys. Lett.* **1990**, *174*, 553−557.
(5) Nie, S. M.; Chiu, D. T.; Zare, R. N. *Science* **1994**, *266*, 1018−1021.
(6) Eigen, M.; Rigler, R. *Proc. Natl. Acad. Sci. U.S.A.* **1994**, *91*, 5740−5747.
(7) Edman, L.; Foldes-Papp, Z.; Wennmalm, S.; Rigler, R. *Chem. Phys.* **1999**, *247*, 11−22.
(8) Ambrose, W. P.; Goodwin, P. M.; Martin, J. C.; Keller, R. A. *Science* **1994**, *265*, 364−367.
(9) Levene, M. J.; Korlach, J.; Turner, S. W.; Foquet, M.; Craighead, H. G.; Webb, W. W. *Science* **2003**, *299*, 682−686.
(10) Lu, H. P.; Xun, L.; Xie, X. S. *Science* **1998**, *282*, 1877−1882.
(11) Kapanidis, A. N.; Lee, N. K.; Laurence, T. A.; Doose, S.; Margeat, E.; Weiss, S. *Proc. Natl. Acad. Sci. U.S.A.* **2004**, *101*, 8936−8941.
(12) Knemeyer, J. P.; Marmé, N.; Sauer, M. *Anal. Chem.* **2000**, *72*, 3717−3724.
(13) Li, H. T.; Ying, L. M.; Green, J. J.; Balasubramanian, S.; Klenerman, D. *Anal. Chem.* **2003**, *75*, 1664−1670.
(14) Castro, A.; Williams, J. G. K. *Anal. Chem.* **1997**, *69*, 3915−3920.
(15) Stephan, J.; Dorre, K.; Brakmann, S.; Winkler, T.; Wetzel, T.; Lapczyna, M.; Stuke, M.; Angerer, B.; Ankenbauer, W.; Foldes-Papp, Z.; Rigler, R.; Eigen, M. *J. Biotechnol.* **2001**, *86*, 255−267.

10.1021/ja042642i CCC: $30.25

high accuracy has not yet been realized. The primary challenge of applying this confocal technique for quantitative analysis is that only a minute fraction of molecules in a solution pass through the miniscule detection volume, leaving a large number of molecules in the solution undetected. The low molecular detection efficiency can either complicate the accuracy in quantification, arising from the stochastic distribution of a low number of molecules within the detection region, or demand prolonged measurement times for achieving high accuracy.

We present here a method capable of quantitative detection of low-abundance DNA/RNA based on confocal single-molecule detection. This method incorporates the use of molecular beacons (MBs)[16,17] to achieve specific DNA detection in a homogeneous assay format, which does not require separation or removal of unbound probes, and an electrode-embedded microfluidic reactor for controlling the transport of DNA molecules. A high molecular detection efficiency is accomplished by rapidly transporting molecules inside a microchannel with a hydrodynamic flow, followed by precise confinement ("focusing") of individual molecules through a minuscule detection region using electric field-induced (electrokinetic) forces. Accurate quantification of a minute quantity of nucleic acids is accomplished by tracing and counting them at the single-molecule level.

Experimental Section

Assay Overview. Detection of specific nucleic acids in solution is carried out using MBs. MBs are hairpin structure oligonucleotide probes that become fluorescent only when hybridized with their complementary sequences (Figure 1A). Since the unbound MBs remain nonfluorescent, removal of unbound probes (through steps of immobilization and wash) to avoid false positive detection becomes unnecessary. The utilization of MBs, therefore, allows detection of nonimmobilized molecules in a solution, enabling detection of specific moving nucleic acids with confocal spectroscopy.

Transporting and focusing molecules through a laser-focused detection region for single-molecule tracing is implemented by an electrode-embedded microfluidic reactor (Figure 1B). A sample solution is introduced at the inlet of a microchannel and then driven through by hydrodynamic pumping. When molecules enter the electrode region, their transport is governed by electrode-controlled electrokinetic forces, which steer them toward the region of minimal energy, located at the center of the middle electrode. The focused laser beam of a confocal fluorescence spectroscope is positioned at the downstream end of the energy minimum region (Figure 1B,C), wherein fluorescent bursts emitted from individual molecules are detected. The amount of target molecules is quantified according to the number of the counted single-molecule fluorescence events.

Microchip Fabrication. The fluidic reactor, comprising a microchannel (5−10 μm in depth and 40 μm in width) and a trio of three-dimensional metal electrodes, was fabricated from a silicon wafer using microfabrication technology. The electrodes consist of two side electrodes extending from the bottom to the upper corners of the microchannel and a middle electrode in the center of the channel bottom. Tapered sidewalls were formed through a silicon anisotropic etch process (with KOH etchant) for better metallic coverage. To electrically isolate the silicon substrate, a 5000 Å silicon dioxide layer was grown using a thermal oxidation furnace. To alleviate the problem of nonuniform exposure involved in patterning electrodes over a microchannel, a 8 μm thick AZ4620 photoresist (PR) (Calriant, Lafayette, LA) was used and overexposed in the lithography process. The PR-coated region defined the nonelectrode area, and the open region was for metal deposition. A 200/2000 Å Cr/Au metal layer was deposited as the electrode material using an evaporation process. A lift-off technique was then applied to remove the portion of metal film on top of the PR by dissolving the PR with acetone, thereby releasing the 3-D electrodes. Two holes on a 160 μm thick Borofloat glass plate (Precision Glass & Optics, Santa Ana, CA) serving as reservoirs for the microchannel were drilled using a 1.2 mm diameter diamond-plated drill bit (McMaster, Atlanta, GA). The predrilled glass plates were spin-coated with UV-curable SU-8 polymer (MicroChem, Newton, MA) and cured at 85 °C for 3 min for the subsequent bonding process. The glass plates were then bonded to the microchannels via the SU-8, and the bonded chips were further cured at 95 °C for 10 min to remove excess solvents. Finally, a photomask was used to limit the SU-8 exposure to the region outside the microchannel, and a SU-8 developer was then introduced to dissolve the nonexposed SU-8 residual inside the microchannel.

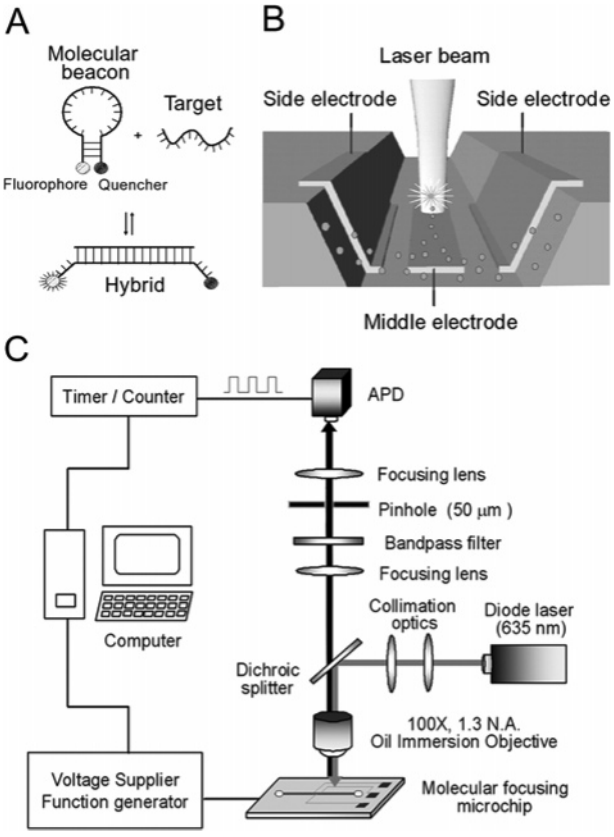

Figure 1. On-chip single-molecule assay for low-abundance nucleic acid detection. (A) The hairpin structure of an MB brings a fluorophore and a quencher in close proximity, causing quenching of fluorescence. Fluorescence is restored when the MB hybridizes with its complementary strand. (B) Schematic representation of molecular focusing in an electro-embedded microchannel. The electrodes consist of two side electrodes and a middle electrode. Upon introduction of an electric potential, the resulting field confines and focuses DNA molecules to a minuscule confocal detection region on top of the middle electrode, downstream in the microchannel. Individual molecules are sequentially excited by a focused laser beam, emit fluorescence, and are counted as they flow through the detection region. (C) Schematic diagram of a confocal fluorescence spectroscope setup and the detection arrangement.

T2 DNA and Fluorescent Beads Preparation. T2 DNA and carboxylate-modified latex (CML) beads were prepared for monitoring in real time the process of particulate focusing through direct visualization. T2 DNA was purchased from Sigma-Aldrich (St. Louis, MO). They were stained with YOYO-1 iodide (Molecular Probes, Eugene, OR), with the base pair/dye molecule ratio kept at 5:1, and were diluted with 1X TBE (Tris/boric acid/EDTA). The resulting solution was then

(16) Tyagi, S.; Kramer, F. R. *Nat. Biotechnol.* **1996**, *14*, 303−308.
(17) Tyagi, S.; Bratu, D. P.; Kramer, F. R. *Nat. Biotechnol.* **1998**, *16*, 49−53.

incubated for 30−60 min at room temperature in the dark and diluted to the desired concentrations before measurements. The 1 μm CML beads, obtained from Interfacial Dynamics Corporation (Portland, Oregon), have negative surface charges and have been preloaded with multiple fluorescence dyes (blue-excitation and green-emission), offering sufficient fluorescence intensity for single-particle observation. The beads were diluted with 1X TBE and were sonicated for 3 min immediately before use to ensure the beads did not coagulate.

Synthesis of MBs and ssDNA Targets. We used synthetic ssDNA as a model target in this on-chip single-molecule detection assay. Both MBs and ssDNA were synthesized and HPLC-purified by Integrated DNA Technologies (Coralville, IA). The nucleotide sequence of the MBs was designed as follows: Cy5-5′-CCTGC CACGG TCTGA GA GGTCG-3′-BHQ-2, where the underlined sequence identifies the nucleotides participating in the formation of the stem. The sequence of the target strand was 5′-TCTCA GACCG TGGCA GG-3′. Powders of MBs and the ssDNA were diluted with DI water and stored at −20 °C. They were further diluted with high salt buffer (10 mM Tris/HCl, 50 mM KCl, 1 mM $MgCl_2$) to the desired concentrations, mixed, and stored at −4 °C overnight before use. The detection was performed at room temperature.

Experimental Setup. Reagents were injected into the microchannel through a tubing connection (polyetheretherketone tubing, Upchurch Scientific, Oak Harbor, WA) and then driven through the flow passage using a syringe pump (Harvard Apparatus, Holliston, Ma). An inverted fluorescence microscope (IX70, Olympus America Inc., Melville, NY) was used for monitoring the movement of T2 DNA and CML beads. The microscope was equipped with a 100 W mercury lamp and a 100X/1.25 N.A. oil immersion objective (Plan Achromat, Olympus America Inc., Melville, NY). The time-serial trajectories of particles were video recorded using an intensified charge-coupled device (CCD) camera (ICCD 350F, Videoscope International, Dulles, VA). A confocal fluorescence spectroscope (Figure 1C) was custom-made to measure the photon histogram in the experiments of single-molecule detection with MBs. In the spectroscope, a 635 nm diode laser (Thorlabs, Newton, NJ) was use to induce fluorescence. A light beam (0.15 mW) from the laser passes into a beam expander and then reflects from a dichroic beam splitter (Chroma Technology, Rockingham, VT) to a 100X/1.30 N.A. oil immersion objective (Plan Fluorite, Olympus America Inc., Melville, NY). The probe volume was approximated to a cylinder, 0.85 μm in diameter and 2 μm in height, which gives a detection volume of about 1.1 fL, based on the standard fluorescence correlation spectroscopy (FCS) measurement of fluorophores (fluorescein) and its curve fitting to the model of thermal diffusion in a Gaussian optical confinement volume.[18]

The emitted fluorescence was collected by the same objective, filtered by a band-pass filter (XF3030, Omega Optical, Brattleboro, VT), focused by a focusing lens, penetrated through a 50 μm pinhole, and finally collected by an avalanche photodiode (SPCM-AQR, Perkin-Elmer, Wellesley, MA). Amplified TTL pulses were counted by a 32-bit counter/timer (PCI 6602, National Instruments, Austin, TX) and stored. A program written in LabView was created to perform data acquisition and to set the bin width (integration time per data point) of counting.

Determination of Statistical Accuracy and Measurement Time. The length of time required for achieving a certain statistical accuracy/confidence level was calculated using Poisson statistics. Poisson distribution for calculating the probability of detecting a specific number of fluorescent bursts in a unit time is given by

$$P(n) = (\lambda t)^n e^{-\lambda t}/n!$$

where $P(n)$ is the probability of events with the number of detected fluorescent bursts, n, in time, t; λ is the mean fluorescent burst rate determined experimentally from either the molecular events (signal) or background. The statistical accuracy/confidence level was calculated by determining the overlap between $P(n)_{signal}$ and $P(n)_{background}$ and subtracting it from 1. The required measurement time was determined by the time allowed to achieve a 99% accuracy/confidence level.

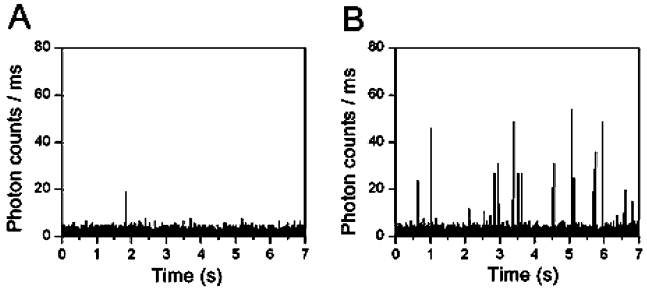

Figure 2. Single-molecule fluorescent signals from MBs. (A) When complementary targets are absent, high intensity fluorescence bursts were rarely detected. (B) After the addition of complementary targets (7 nM), an increased number of fluorescent bursts were detected. The concentration of MBs was 70 pM.

Results and Discussion

Detecting Specific Sequences with MBs. Figure 2 depicts two 7 s representative fluorescent signals of MBs (70 pM) in the absence and presence of complementary ssDNA targets, detected with a confocal fluorescence spectroscope. When detecting low-concentration fluorescent molecules (<1 nM), the detected fluorescent signals are discrete because the molecular occupancy (the average number of molecules residing in the ~1 fL detection volume) is smaller than unity, and a burst of fluorescence photons is emitted when a fluorescent molecule passes through the detection volume. As shown in Figure 2A, MBs rarely exhibit enough fluorescence intensity to be unambiguously detected. This control shows that only a minute subpopulation of unbound MBs had unraveled into fluorescent random coils under thermal fluctuations. A similar result (data not shown) was also obtained when measuring MBs in the presence of noncomplementary targets, suggesting that the MBs did not hybridize to the noncomplementary targets. When complementary targets were introduced causing the hairpin structure of MBs to unfold, a corresponding increase in the number of fluorescent bursts was seen (Figure 2B). The average fluorescence intensity (photon count rate) of fluorescent bursts was 17.8 photon counts/ms against an average background intensity of 0.85 photon counts/ms, achieving a high SNR of ~20. In comparison with conventional ensemble methods, where the SNR decreases with the target concentration, the SNR of single-molecule fluorescent bursts is independent of concentration. Thus, the high SNR can still be retained even at extremely low concentration levels when using the confocal single-molecule technique for analysis.

Characterization of Molecular Focusing Chip. To investigate the process of particulate focusing in the electrode-embedded microchip, fluorescently labeled T2 DNA (164 Kbp) and CML beads (1μm) were used to conduct particulate manipulation experiments. Both particles provide sufficient fluorescence intensity for single-particle visualization, so that the characterization of the focusing process could be accomplished by observing in real-time the trajectories of individual particles under the influence of a controlled electric field.

A combined dc and ac potential (10 kHz, 1.4 V peak−peak with 0.7 V offset) was applied between the two side electrodes

(18) Rigler, R.; Mets, U.; Widengren, J.; Kask, P. *Eur. Biophys. J.* **1993**, *22*, 169−175.

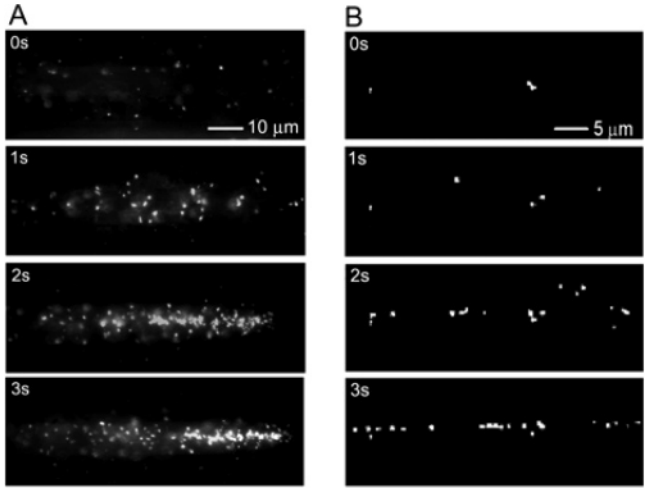

Figure 3. Time-serial epifluorescence images of the process of focusing T2 DNA and CML beads in a microchannel. (A) Flowing T2 DNA were gradually focused to the center of the downstream microchannel after a potential was applied. (B) CML beads in a stationary solution were confined and lined up in the center of the microchannel.

(cathode) and the middle electrode (anode) to induce both electrophoresis (EP) and dielectrophoresis (DEP)[19−21] for manipulating T2 DNA. Charged particles experience an electrostatic EP force under the influence of a dc field; whereas, particles (charged or neutral) in an inhomogeneous ac field are subjected to a DEP force when polarized with respect to its surrounding medium. The applied potential produced a DEP force that moved DNA to regions of maximum field strength at the edges of the middle electrode. Due to the DNA's intrinsic negative charge, DNA molecules were simultaneously attracted toward the middle electrode by an EP force induced by the dc component of the applied potential. Since the lateral electric field was zero at the center of the middle electrode, DNA molecules attracted to this region were not subjected to lateral electrostatic forces and thus were confined herein. A process of T2 DNA focusing is shown in the time-serial epifluorescence images in Figure 3A. Prior to applying an electric field, DNA molecules were randomly distributed throughout the microchannel. Thus, the only observable DNA molecules were a fraction of the total that dwelled on the focal plane in proximity to the bottom of the microchannel. Immediately after the potential was applied, DNA molecules were directed from the top and side regions of the microchannel toward the center of the middle electrode while they were flowing downstream. The gradual increase of observed DNA molecules in the focal plane was the result of molecules moving from higher out-of-focus regions to the lower focal region at the middle electrode. Since the molecules passing through the end of the electrode region had been exposed to the electrical field for a longer time period than those molecules that had just entered the electrode region, the DNA downstream of the microchannel were more narrowly confined. Hence, the molecular detection efficiency of confocal fluorescence spectroscopy can be best enhanced when the detection is performed at the downstream end of the middle electrode.

(19) Wong, P.; Wang, T. H.; Deval, J.; Ho, C. H. *IEEE/ASME Trans. Mechatron.* **2004**, *9*, 366−376.
(20) Pohl, H. A. *J. Appl. Phys.* **1951**, *22*, 869−871.
(21) Ramos, A.; Morgan, H.; Green, N. G.; Castellanos, A. *J. Phys. D: Appl. Phys.* **1998**, *31*, 2338−2353.

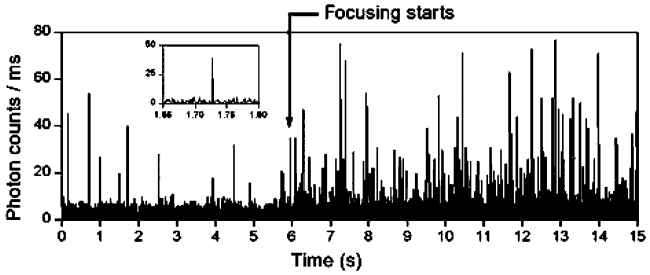

Figure 4. Tracing moving MB−target hybrids in a microchannel before and after introduction of an electric potential. The measured solution contained a mixture of MBs (70 pM) and a 10-fold excess of targets. The electric potential was applied at $t = 6.0$ s, causing a significant increase in fluorescent burst count rate.

CML beads were prepared for observing particle trajectories for a longer time period during the manipulation process since they have better photostability against photobleaching. The time-serial epifluorescence images in Figure 3B present the course of focusing CML beads in a stationary solution inside a microchannel. Similar to the process of manipulating T2 DNA, beads gradually entered the middle electrode region after a combined dc and ac potential (100 kHz, 1.0 V peak−peak with 0.5 V offset) was applied. In contrast to T2 DNA manipulation, where the molecules are embedded in a continuous flow, the CML beads resided in a stationary solution so that the time that they had been exposed to the electric field was independent of their positions in the longitudinal direction. Consequently, the beads were confined and lined up along the center line of the middle electrode. A movie of the complete focusing process can be found in the Supporting Information.

Tracing and Counting Single DNA Molecules. Figure 4 shows a 15 s trace of fluorescent bursts from a mixture of MBs and DNA targets, detected with a confocal spectroscope on a fluidic microchip. Upon the application of a focusing potential (2 MHz, 1.0 V peak−peak with 1.0 V offset) at $t = 6.0$ s, the rate of fluorescent bursts significantly increased (by ∼25-fold), a result of more molecules, which would otherwise bypass the detection region, being directed through the detection volume. It should be noted that the transport of the hybrids could barely be controlled when the dc component of the applied potential was lower than 0.6 V, regardless of both the frequency and the peak−peak voltage amplitude of the ac potential. The fact that the ac field plays a less significant role in manipulating such small oligonucleotides can be attributed to the decrease in the magnitude of dielectric force as the size of molecules subjected to the field decreases.[20]

Events of fluorescent molecules flowing through the laser-focused detection volume were counted, molecule by molecule, with a threshold of 10 photon counts/ms. The flow speed was adjusted so that the average burst duration, which corresponds to the time a molecule takes to pass through the illumination region, was ∼3 times that of the bin time of photon counting (1 ms). Under these parameters, the average background burst count rate of MBs (70 pM) was 1.35 s^{-1}, measured in the absence of targets. The detected burst count rate increased with the concentration of targets. The relationship between the burst count rate and the target concentration is plotted in Figure 5. A dynamic of range of 4 orders of magnitude was achieved. The fluorescence signal measured at a target concentration as low as 0.7 pM can still be effectively distinguished from the background. The lowest detectable concentration level is limited

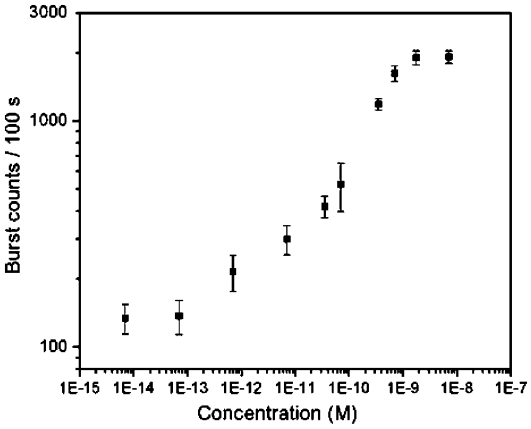

Figure 5. Graphical representation of fluorescent burst count rates as a function of the complementary target DNA concentrations. The concentration of MBs used for detection was kept at 10 pM for each measurement. The error bars result from five independent measurements.

by inefficient hybridization between MB probes and targets, caused by the reduced diffusion-limited forward binding rate constant at such low concentrations.[22] Consequently, this limit can be further lowered by adding more MBs to deplete the unbound DNA targets, while optimizing the design of MBs, hybridization temperature, and salt concentration to suppress the background from the excess MBs.

Detection Time and Accuracy. The accuracy in biomolecule quantification with ensemble fluorescence detection tends to be complicated by the fluorescence variability caused by photobleaching, storage of fluorophores, and buffer conditions, such as the salt concentrations and pH values.[23−25] This issue is particularly significant when the analytes to be detected are low-abundant due to the decreased SNR and relatively high signal variances with respect to the background noise level. In contrast, when using single-molecule detection for quantitative analysis, the amount of targets is quantified according to the number of the single molecules being detected. Each single-molecule fluorescent burst has a high SNR, which is independent of the quantity of molecules in solutions. In addition, the stochastic variance in molecular counting decreases with the increased number of molecules counted. Consequently, high accuracy in quantification of low-concentration targets can be achieved by allowing sufficient times for molecular counting. Figure 6 shows the measurement times needed to achieve a 99% accuracy/confidence level for quantitatively detecting targets without complications from the background noises at different concentrations, calculated by Poisson statistics (see Experimental Section), according to the average background burst count rate and the average detected burst count rate after the targets are added (see Table S1 in the Supporting Information). Less than 1 s is required to achieve a 99% accuracy/confidence level when detecting targets of a concentration higher than 0.7 nM. By extending the measurement time to ∼90 s, detection with the same level of accuracy can still be accomplished when the target concentration is only 0.7 pM.

To address the reduction in analysis time by the application of the molecular focusing technique, the time required for detection in the absence of molecular focusing was also determined, as shown in Figure 6, for comparison. With an enhanced molecular count rate by molecular focusing, detection can be completed within a much shorter time period. For example, when detecting a solution containing 70 pM targets, the measurement can be completed within 4 s when an electric potential was applied to focus molecules to the detection region; whereas, ∼200 s is required for detection in the absence of molecular focusing.

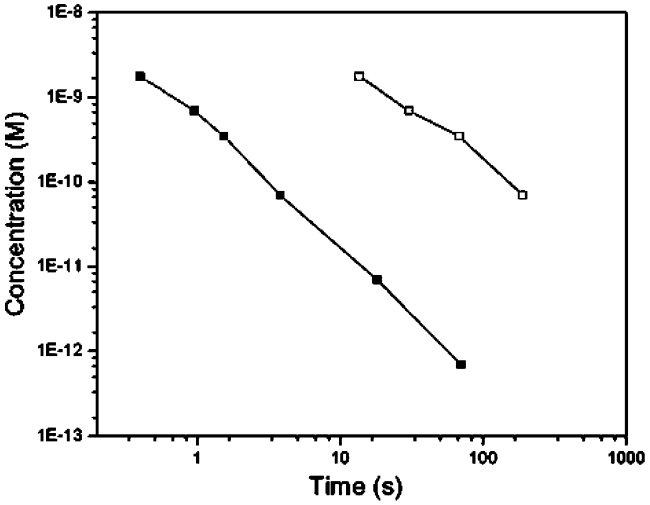

Figure 6. Plot of the relationship between the concentration of targets and the measurement time required for achieving 99% accuracy/confidence level. With single-molecule detection, highly accurate detection at a lower target concentration level can be accomplished by elongating the measurement time. Detection with molecular focusing (■) requires a much shorter measurement time for achieving the 99% accuracy/confidence level at a given concentration and achieves a lower concentration detection limit with a given measurement time, as compared with the case of detection without molecular focusing (□).

By detecting molecules in a continuous-flow manner inside a fluidic microchannel, the photobleaching effect was prevented (see Figure S1 in the Supporting Information) because each molecule rapidly flows into and leaves the laser illumination region only once, and the time that a molecule stays in the detection region is only ∼3 ms. This allows the on-chip single-molecule assay to extend the measurement time to increase detection accuracy without complications caused by photobleaching.

Conclusions

We have shown in this work that the single-molecule approach provides a more effective and accurate way for quantitative analysis of low-abundance nucleic acids than the conventional ensemble methods. However, successful implementation of confocal single-molecule detection for quantitative applications requires integration of an effective molecular transport and confinement mechanism. A number of particle confinement techniques have been developed and used in flow cytometry and capillary electrophoresis, including hydrodynamic focusing,[26,27] electric-current focusing,[28−30] and physical

(22) Calef, D. F.; Deutch, J. M. *Annu. Rev. Phys. Chem.* **1983**, *34*, 493−524.
(23) Chen, Y.; Dougherty, E. R.; Bittner, M. L. *J. Biomed. Opt.* **1997**, *2*, 364−374.
(24) Sagner, G.; Goldstein, C.; Miltenburg, R. *Biochemica* **1999**, *2*, 7−11.
(25) Van Dyke, K.; Van Dyke, C.; Woodfork, K. *Luminescence Biotechnology Instruments and Applications*; CRC Press: New York, 2001.
(26) Nguyen, D. C.; Keller, R. A.; Jett, J. H.; Martin, J. C. *Anal. Chem.* **1987**, *59*, 2158−2161.
(27) Castro, A.; Fairfield, F. R.; Shera, E. B. *Anal. Chem.* **1993**, *65*, 849−852.
(28) Jacobson, S. C.; Ramsey, J. M. *Anal. Chem.* **1997**, *69*, 3212−3217.
(29) Schrum, D. P.; Culbertson, C. T.; Jacobson, S. C.; Ramsey, J. M. *Anal. Chem.* **1999**, *71*, 4173−4177.
(30) Haab, B. B.; Mathies, R. A. *Anal. Chem.* **1999**, *71*, 5137−5145.

confinement.[30−32] Although effective in those applications, the use of these available confinement methods for confocal single-molecule detection poses several complications, such as the off-center focusing (in the hydrodynamic and electric-current focusing techniques) as well as channel clogging and high levels of background noise caused by increased reflection from surfaces (in the physical confinement technique).

Herein, we used the combined EP and DEP, induced via a trio of 3-D microelectrodes, to achieve confinement of small oligonucleotides (27 bp MB probes and 17 bp DNA targets) to a submicron detection region. This electrokinetic molecular focusing technique enables efficient and precise molecular confinement, therefore, allowing the use of a relatively larger flow passage both to ensure enough separation between the detection region and the channel sidewalls and to increase the throughput of analysis, rendering the technique ideal for confocal fluorescence detection.

The on-chip single-molecule assay, which was realized by the use of MBs, a molecular focusing microchip, and confocal spectroscopy, provides several advantages over the conventional methods. Detection is performed without the need to remove unbound probes. A minimal sample amount of 20 nL is required for analysis (calculated according to the setting volume flow rate of 0.2 nL/s for a measurement time course of 100 s), thereby achieving a detection limit of ∼14 zmole. Moreover, the amount of MBs used in this chip-based single-molecule assay is only ∼1.4 amole, which is about 7 orders of magnitude less than that used in the ensemble methods, such as real-time PCR.[17,33] Since the consumption of molecular probes usually accounts for a great part of the total cost in hybridization-based detection assays, the significant reduction in probe consumption achieved by this method renders it a very cost-effective approach for nucleic acid detection.

Acknowledgment. This work was supported by DARPA (N66001-00-c-8092), NSF (DBI-0352407), and Whitaker Foundation.

Supporting Information Available: The process of on-chip electrokinetic focusing in real-time, burst count rates before and after target addition, photobleaching effect (MOV and PDF). This material is available free of charge via the Internet at http://pubs.acs.org.

JA042642I

(31) Lee, Y. H.; Maus, R. G.; Smith, B. W.; Winefordner, J. D. *Anal. Chem.* **1994**, *66*, 4142−4149.
(32) Lyon, W. A.; Nie, S. M. *Anal. Chem.* **1997**, *69*, 3400−3405.
(33) Vet, J. A. M.; Majithia, A. R.; Marras, S. A. E.; Tyagi, S.; Dube, S.; Poiesz, B. J.; Kramer, F. R. *Proc. Natl. Acad. Sci. U.S.A.* **1999**, *96*, 6394−6399.